

---

# On the statistical detection of propagating waves in polar coronal hole

G. R. Gupta<sup>1,2</sup>, E. O'Shea<sup>3</sup>, D. Banerjee<sup>1</sup>, M. Popescu<sup>3</sup>, and J. G. Doyle<sup>3</sup>

<sup>1</sup> Indian Institute of Astrophysics, Bangalore, India

<sup>2</sup> Indian Institute of Science, Bangalore, India

<sup>3</sup> Armagh Observatory, College Hill, Armagh, N. Ireland

**Summary.** Waves are important for the heating of the solar corona and the acceleration of the solar wind. We have examined a long spectral time series of a southern coronal hole observed on the 25th February 1997, with the SUMER spectrometer on-board SoHO. The observations were obtained in a transition region N IV 765 Å line and in a low coronal Ne VIII 770 Å line. Our observations indicate the presence of compressional waves with periods of 18 min. We also find significant power in shorter periods. Using Fourier techniques, we measured the phase delays between intensity as well as velocity oscillations in the two chosen lines over a frequency domain. From this we are able to measure the travel time of the propagating oscillations and, hence, the propagation speeds of the waves producing the oscillations. As the measured propagation speeds are subsonic, we conclude that the detected waves are slow magneto-acoustic in nature.

## 1 Introduction

Coronal holes are regions of cool and low density plasma that are 'dark' at coronal temperatures. The predominantly unipolar magnetic field from coronal hole regions is thought to give rise to the fast solar wind. A number of studies e.g., Ofman et al. 1997, 2000; Banerjee et al. 2001; Popescu et al. 2005 have measured oscillations in coronal holes in the polar off-limb regions of the Sun. All of these studies point to the presence of compressional waves, thought to be slow magnetoacoustic waves as found by Deforest & Gurman (1998); O'Shea et al. (2006, 2007). Recently, Gupta et al. (2009) have reported on the detection of these waves on the disk part of the coronal hole. They also find a different nature of compressional waves in bright (network) and dark (internetwork) regions of polar coronal hole (here after pCH). In this short contribution we extend the same analysis for another dataset. For further details please refer to Gupta et al. (2009).

## 2 Observations and data analysis

Data used for this analysis was taken on 25th February 1997, from 00:00 UT to 13:59 UT with the  $1 \times 300''$  slit on SUMER, and with an exposure time of 60 sec, in N IV 765 Å and Ne VIII 770 Å lines in a southern coronal hole. For details on data reduction please refer to Gupta et al. (2009). The Chromosphere and Transition Region show a network (and cell/internetwork) pattern, with intensity enhancements in the network boundaries. Presumably, the magnetic field is predominantly concentrated on such network boundaries and, within coronal holes, the footpoints of coronal funnels emanate from these network boundaries. As the duration of the observation in this dataset is very long, the location of bright and dark pixels along the slit will change with time. For this reason, we have analysed the whole dataset pixel by pixel and timeframe by timeframe. For example, for one time instance we first calculate

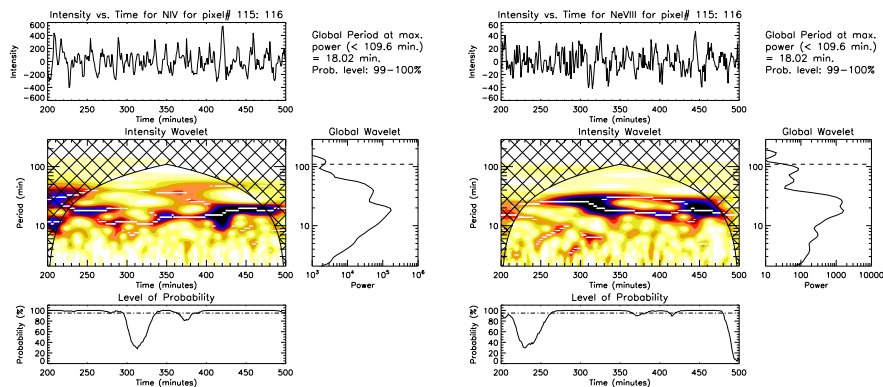


**Fig. 1.** The wavelet result for a bright location (pixel no. = 115 – 116 which corresponds to  $Y \approx -915''$ ) in the N IV and Ne VIII intensity. In each set the top panels show the relative (background trend removed) radiant flux, the central panels show the colour inverted wavelet power spectrum, the bottom panels show the variation of the probability estimate associated with the maximum power in the wavelet power spectrum (marked with white lines), and the right middle panels show the global (averaged over time) wavelet power spectrum. Above the global wavelet the period, measured from the maximum power from the global wavelet, together with probability estimate, is printed.

the average intensity along the slit. All pixels having an intensity higher than 1.25 times this average intensity were chosen as bright pixels. If, this pixel is bright for at least 60 min (or 60 timeframes), then that pixel is considered to be a bright (‘network’) location over that time interval. The bright pixel identification is done only for the low temperature N IV line; the network pixels obtained from it are assumed to be the same in the higher temperature Ne VIII line.

### 3 Results and Discussions

In Fig. 1, we show a representative example of the type of oscillations measured in a bright region of the pCH using wavelets, which provides information on the temporal variation of a signal (Torrence & Compo 1998). Further details on the wavelet analysis used here can be found in Gupta et al. 2009; O’Shea et al. 2001 and reference therein. From Fig. 1, we can see oscillations of  $\approx 18$  min period in both lines at the same location. This gives an indication that these two layers are linked. A propagating wave passing from one layer to the other could explain this finding. To test this hypothesis and to find the nature of the propagating waves, we measure the phase delays in intensity and also in the LOS relative velocity between both lines for each of the measurable pixels along the slit for a full frequency range. This work has followed the method used by Athay & White (1979); O’Shea et al. (2006) and Gupta et al. (2009) which make use of the basic equation of phase delay,  $\Delta\phi = 2\pi fT$  where  $f$  is the frequency and  $T$  the time delay in seconds. From this relation, we expect the phase difference will vary linearly with  $f$ , and will change by  $360^\circ$  over frequency intervals of  $\Delta f = 1/T$ . This will give rise to parallel lines in  $\Delta\phi$  vs.  $f$  plots at fixed frequency intervals ( $\Delta f = 1/T$ ), corresponding to a fixed time delay  $T$ . The method used here to identify the parallel lines in the phase plot

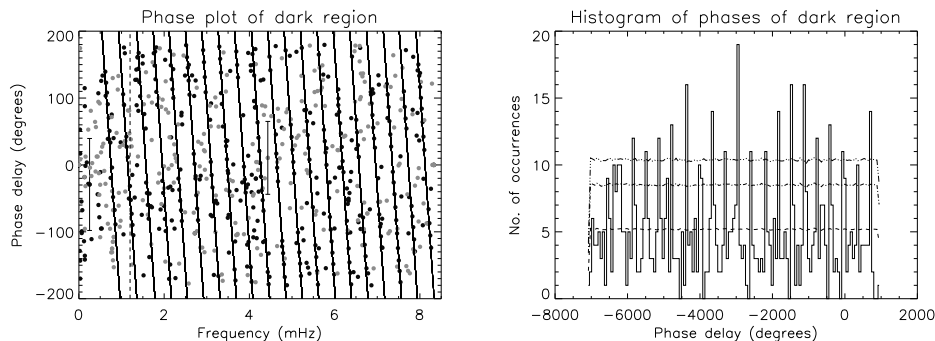


**Fig. 2.** Left panel: Phase delays measured between the oscillations in the spectroscopic line pair for dark locations. The phases from radiant flux oscillations are shown as the grey circle symbols while those from LOS velocities are shown as the black circle symbols. Overplotted on each figure are black parallel lines, corresponding to fixed time delays. The vertical dashed line drawn at 1.2 mHz indicates that some phase values below this could be affected by solar rotation. Representative errors on the phase measurements are indicated by the error bars. Right panel: Histogram showing the distribution of phase delay measurements as a function of frequency for the dark locations. The horizontal dotted, dot-dashed and long dashed lines show the 68.3% (i.e.,  $1\sigma$ ), 90% ( $\approx 1.64\sigma$ ) and 95% ( $\approx 2\sigma$ ) confidence levels, respectively, calculated using Monte-Carlo simulations with 5000 permutations.

(left panel of Fig. 2) and the histogram (right panel of Fig. 2), generated to obtain the spacing between the lines and their significance level, is discussed in greater detail in Gupta et al. (2009). In the bright location, we didn't have enough statistics to come to a reliable conclusion. Because of space constraints we do not show the corresponding plots for the bright region here. Whereas oscillations were detected within the dark internetwork locations also and the statistics is much better and we show the results here in Fig. 2.

In the dark locations of pCH (left panel of Fig. 2), we measured a time delay of  $-2607 \pm 491.2$  s between the two lines, indicating upwardly propagating waves. Notice the many closely spaced, steeply sloped, parallel phase lines that correspond to this long time delay. In right panel of Fig. 2 these parallel phase lines correspond to significant peaks above 95% significance in the histogram. Here, the peaks are equally spaced at the phase difference of  $360^\circ$  that would be expected for unimpeded propagating waves.

The measured time delays from the pCH may be used to estimate propagation speeds for the waves assumed to be causing the oscillations. In order to calculate the propagation speeds, one needs information on the height difference in the atmosphere between the different lines in the line pair. The height difference of 4095 km has been calculated using the limb brightening technique as described in O'Shea et al. (2006); Gupta et al. (2009). Using this height difference and the measured time delay, we find a speed of  $-1.6 \pm 0.3$  km s<sup>-1</sup> for the dark region which is less than the acoustic velocity at that height. Hence, the identified waves can be termed as slow magento-acoustic waves. These waves are rather slow and may not carry enough energy flux for the acceleration of the solar wind.

## References

- Athay, R. G. White, O. R. 1979, ApJ, 229, 1147  
 Banerjee, D., O'Shea, E., Doyle, J. G., Goossens, M. 2001, A&A, 380, L39  
 Deforest, C. E. Gurman, J. B. 1998, ApJ, 501, L217+  
 Gupta, G. R., O'Shea, E., Banerjee, D., Popescu, M., Doyle, J. G. 2009, A&A, 493, 251  
 Ofman, L., Romoli, M., Poletto, G., Noci, G., Kohl, J. L. 1997, ApJ, 491, L111+  
 Ofman, L., Romoli, M., Poletto, G., Noci, G., Kohl, J. L. 2000, ApJ, 529, 592  
 O'Shea, E., Banerjee, D., Doyle, J. G. 2006, A&A, 452, 1059  
 O'Shea, E., Banerjee, D., Doyle, J. G. 2007, A&A, 463, 713  
 O'Shea, E., Banerjee, D., Doyle, J. G., Fleck, B., Murtagh, F. 2001, A&A, 368, 1095  
 Popescu, M. D., Banerjee, D., O'Shea, E., Doyle, J. G., Xia, L. D. 2005, A&A, 442, 1087  
 Torrence, C. Compo, G. P. 1998, Bulletin of the American Meteorological Society, 79, 61